

Sano–Tachiya–Noolandi–Hong versus Onsager modelling of charge photogeneration in organic solids

K. Falkowski^{a,b}, W. Stampor^{a,*}, P. Grygiel^a, W. Tomaszewicz^a

^a Department of Electronic Phenomena, Faculty of Applied Physics and Mathematics, Gdańsk University of Technology, Narutowicza 11/12, 80-233 Gdańsk, Poland

^b Department of Atomic Physics and Luminescence, Faculty of Applied Physics and Mathematics, Gdańsk University of Technology, Narutowicza 11/12, 80-233 Gdańsk, Poland

ARTICLE INFO

Article history:

Received 4 August 2011

In final form 26 October 2011

Available online 17 November 2011

Keywords:

Charge photogeneration
Onsager model
Geminate recombination
Organic solids
Electromodulation
OLEDs
Alq₃
Iridium complex

ABSTRACT

We have studied the electric field dependence of charge photogeneration efficiency in organic solids for various radial distribution functions (Dirac delta, Gaussian, exponential) of initial e–h pairs in the framework of Sano–Tachiya–Noolandi–Hong (STNH) theory assuming that the final recombination (capture reaction) proceeds on a sphere of finite radius (a) with a finite velocity (κ). We compare the STNH results with the conventional Onsager theory assuming $a = 0$. We show that charge photogeneration is more enhanced, especially in low-electric field range, for broader initial pair distributions and for smaller final recombination velocities. We compare theoretical results with experimental data taken from electromodulation of photoluminescence (EML) for two archetypical organic photoconductors, Alq₃ and Ir(ppy)₃, commonly used as emitters in organic LEDs. From analysis of our results we infer the lower limit of final recombination velocity, $\kappa = 0.2$ – 2 cm/s, in vacuum evaporated films of Alq₃ and Ir(ppy)₃ which compares favorably with an evaluation of this quantity in amorphous solids.

© 2011 Elsevier B.V. All rights reserved.

1. Introduction

Absorption of light in organic solids leads to creation of excited states (excitons) which may dissociate to form free charge carriers. Taking into account a large Coulombic interaction radius ($r_c > 10$ nm) in these low mobility materials the charge photogeneration is commonly assumed to proceed via an intermediate state of bound electron–hole pairs (geminate e–h pairs or CT states) in which electron and hole, attracted to each other by the Coulomb forces, are separated to a distance (r_0) of one or several lattice constants [1,2]. The schematic diagram in Fig. 1 concerns exciton dissociation and photogeneration of charge carriers when optical excitation occurs in the spectral range of singlet exciton transition in a typical fluorescent organic photoconductor. It is assumed that a hot Franck–Condon molecular exciton state S^* after its autoionization dissipates its excess energy by scattering with the medium and decays to a thermalized bound (e–h) pair or – via internal conversion and vibrational relaxation – reaches the emissive relaxed exciton S_1 state. This state in turn undergoes the non-radiative or radiative (fluorescence) decay to the ground S_0 state. The (e–h) pair dissociates to free charge carriers with probability Ω (escape probability) or – as a result of geminate recombination (with R

probability) re-generates the S_1 state. According to this scheme, the efficiency of charge photogeneration can be expressed as

$$\eta = \eta_0 \Omega, \quad (1)$$

where η_0 is the primary yield of geminate pair formation. In most widely used models of charge photogeneration premised on Onsager [3–5] and Poole–Frenkel (PF) [6,7] theories of geminate recombination it is assumed that η_0 is independent of electric field and electric field dependence of escape probability Ω controls charge photogeneration process [1,2].

Thus, the electric field applied to the sample, by increasing the escape probability Ω of (e–h) pairs, leads to the increase in free carrier production and to the decrease in concentration of S_1 excitons. This is experimentally observed as photocurrent and electric-field-assisted quenching of photoluminescence, respectively. Accordingly, two methods are available to investigate the mechanism of exciton dissociation and carrier photogeneration: the measurement of photocurrent and measurement of photoluminescence in presence of electric field. However, the interpretation of experimental outcomes obtained by the first technique is somehow difficult. In particular, one has to consider some processes affecting the charge carrier transport (e.g. charge trapping and dependence of carrier mobility on electric field strength) as well as the near-electrode processes (optical charge injection). The second method, electromodulated photoluminescence (EML), enables to investigate in a more direct manner dissociation of excitons and charge

* Corresponding author. Tel.: +48 583472704; fax: +48 583472821.

E-mail address: waldek@mif.pg.gda.pl (W. Stampor).

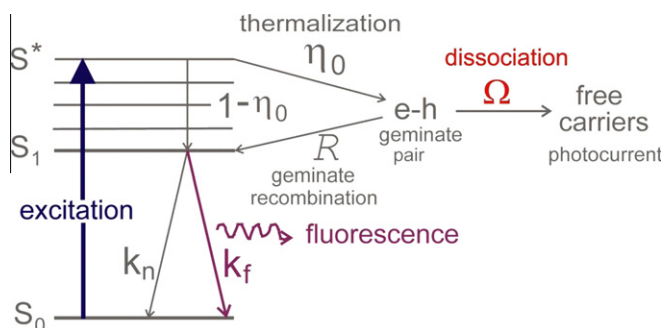


Fig. 1. Schematic diagram of energy levels and photophysical processes involved in photogeneration of charge in a typical organic photoconductor.

separation mechanism in organic solids (for surveys of literature on this subject see references [8–10]).

In some different from Onsager and PF approaches the field dependence of primary quantum yield, η_0 , is also taken into account (see for example references [10,11]). The validity of the basic assumption of the Onsager and PF theories that the η_0 is electric field independent has been widely discussed recently by Arkhipov and Bässler [10] in their comparative study of charge photogeneration in conjugated polymers. This question was also considered in the context of classical Marcus theory of electron transfer [12,13]. According to this reasoning, in single component molecular systems this assumption is not generally fulfilled, in particular, if exciton dissociation starts not from hot exciton S^* state as assumed in Fig. 1 but rather from relaxed S_1 state implying the formation of e–h pair to be electric field dependent.

The classical treatment of e–h separation process by Onsager [3–5] and Sano–Tachiya–Noolandi–Hong (STNH) [14,15], based on solving the Smoluchowski equation, refers to the Brownian random walk of an ion pair in the continuous medium in the presence of an applied electric field. In the STNH model the final geminate recombination step (carrier capture) proceeds on a sphere of finite radius (a) with a finite velocity (κ). The commonly used Onsager theory based on his paper [5] is a special case of a more general STNH treatment for $a = 0$.

In this paper we have studied the electric field dependence of the overall quantum efficiency of charge photogeneration (η) for various distribution functions (Dirac delta, Gaussian, exponential) of the initial distances of e–h pairs in the framework of Sano–Tachiya–Noolandi–Hong model [14,15]. Our approach is essentially very similar to that previously presented by Pan and Haarer [16] with an exception that instead of the conventional Onsager theory the more general STNH theory is applied in our case. We compare our theoretical results with experimental data obtained by EML method for two archetypical organic photoconductors, Alq₃ [17,18] and Ir(ppy)₃ [19], commonly used as emitters in organic light-emitting diodes [20]. We predict the lower limit of final recombination velocity (quenching velocity), $\kappa = 0.2$ – 2 cm/s, in vacuum evaporated layers of Alq₃ and Ir(ppy)₃ which is in good accordance with an evaluation of this quantity in amorphous solids [21,22].

2. Sano–Tachiya–Noolandi–Hong (STNH) and Onsager theory

The escape probability Ω is defined as the probability for the escape of a charge carrier from its parent countercharge. To determine the escape probability Onsager [3–5] and Sano–Tachiya–Noolandi–Hong [14,15] solved the time-independent diffusion (Smoluchowski) equation

$$\text{div} \mathbf{j} = G\delta(\mathbf{r} - \mathbf{r}_0), \quad (2)$$

$$\mathbf{j}(\mathbf{r}) = -D \exp(-W) \text{grad}[\exp(W)\rho]. \quad (3)$$

Here, \mathbf{r} denotes the position of the carrier relative to the countercharge, $\rho(\mathbf{r}|\mathbf{r}_0)$ – the pair distribution function assuming an initial separation \mathbf{r}_0 between particles, G – generation rate of initial pairs, \mathbf{j} – the current density, D – the relative diffusion coefficient ($D = D_1 + D_2$). Under the joint influence of external electric field \mathbf{E} and Coulombic electric field of the countercharge the potential energy, divided by $k_B T$, is given by

$$W(\mathbf{r}) = -\left(\frac{r_c}{r} + 2F\mu\frac{r}{r_c}\right), \quad (4)$$

where

$$r_c = \frac{e^2}{4\pi\epsilon_0\epsilon_r k_B T} \quad (5)$$

is Coulomb interaction (Onsager) radius at which the electron–hole potential energy equals to carrier thermal energy $k_B T$, and

$$F = \frac{eEr_c}{2k_B T} \quad (6)$$

is a dimensionless quantity which gives a measure of the external electric field. Here, e is the magnitude of elementary charge, $\epsilon_0\epsilon_r$ is the electric permittivity of the medium, k_B is the Boltzmann constant and T is the absolute temperature. A frame of reference was chosen such that a drift velocity of the carrier is directed along the positive z axis, so that $\mu = \cos\Theta$ with Θ being the angle between the radius vector and the z axis. In the STNH approach [14,15] the diffusion Eq. (2) is subject to the following boundary conditions:

$$\lim_{r \rightarrow \infty} \rho(\mathbf{r}|\mathbf{r}_0) = 0, \quad (7)$$

$$j_r = -\kappa\rho \text{ for } r = a, \quad (8)$$

where j_r is the radial component of the current density. The boundary condition (8) corresponds to a finite surface recombination velocity κ on a sphere of radius a . If the charge pair is initially positioned at (r_0, Θ_0) the escape probability is then given by

$$\Omega(r_0, \Theta_0) = 1 + 2\pi a^2 G^{-1} \int_{-1}^1 d\mu j_r(a, \mu). \quad (9)$$

After Onsager [3–5], in solving for Ω one can bypass the solution for $\rho(\mathbf{r}|\mathbf{r}_0)$ and obtain the escape probability directly from the equation, $\text{div}_0[\exp(-W(\mathbf{r}_0))\text{grad}_0\Omega(\mathbf{r}_0)] = 0$,

which is adjoint to Smoluchowski Eq. (2). Now, the boundary conditions, relevant to the escape probability Ω , expressed in terms of r_0 become

$$\Omega(r_0 = \infty) = 1, \quad (11)$$

$$D \frac{\partial \Omega}{\partial r_0} = \kappa \Omega \text{ for } r_0 = a \quad (12)$$

Eq. (10), together with the boundary conditions (11) and (12), gives a general method for calculating the escape probability in diffusion (D) and final recombination (κ) controlled e–h separation process. The exact solution for Ω derived by Noolandi and Hong [15] and independently in a more comprehensive manner by Sano and Tachiya [14] involves fairly tedious and time-consuming mathematical manipulations, and therefore a special solution of Eq. (10) for $a = 0$ given by Onsager [5] is usually applied to describe charge photogeneration in organic solids [1,2].

3. Numerical procedures

The initial intrapair separation \mathbf{r}_0 may statistically follow a certain spatial distribution function. From now on, we will drop the

subscript from \mathbf{r}_0 , and denote the initial separation by \mathbf{r} . If $g(r, \theta)$ represents the initial distribution of pair separations, the averaged escape probability can be obtained by integration,

$$\Omega = \frac{\eta}{\eta_0} = \int \Omega(r, \theta) g(r, \theta) d\tau, \quad (13)$$

where $d\tau$ is the volume element. In the present paper we have used the following isotropic distribution functions:

$$g(r, \theta) = \frac{1}{4\pi r^2} \delta(r - r_0), \quad (14)$$

$$g(r, \theta) = g_0 \exp\left(-\frac{(r - r_0)^2}{b^2}\right), \quad (15)$$

$$g(r, \theta) = g_0 \exp\left(-\frac{|r - r_0|}{b}\right), \quad (16)$$

where r_0 is the mean intrapair distance, b is the width of the distribution and g_0 is the relevant normalization factor. The expressions for escape probability $\Omega(r, \theta)$ are as follows.

In the Onsager approach [5]:

$$\Omega(r, \theta) = \exp(-A) \exp(-B) \sum_{n=0}^{\infty} \sum_{m=0}^{\infty} \frac{A^m}{m!} \frac{B^{m+n}}{(m+n)!}, \quad (17)$$

where

$$A = \frac{r_c}{r_0}, \quad B = \frac{Fr_0}{r_c} (1 + \mu). \quad (18)$$

In the STNH approach [14,15],

$$\Omega(r, \theta) = 1 - \sqrt{\frac{r_c}{2r}} \exp\left(\frac{W(r, \theta)}{2}\right) \sum_{l=0}^{\infty} \beta_l Z_l^2\left(\frac{2r}{r_c}\right) T_l(\theta). \quad (19)$$

Here Z_l^2 stands for the Z special function of the second kind of l order which can be expressed as a relevant linear combination of Bessel functions [15] and T_l is the generalized Legendre function of l order defined and investigated by Onsager [4]. The calculation of β_l coefficients and evaluation of special functions were performed using standard numerical procedures [23]. In particular, solving a set of corresponding linear equations was realized by Jacobi method [24].

The basic features of the models and their symbols used in the present paper are collected in Table 1. The analytical expressions for averaged escape probability $\Omega(F)$ are available for models assuming an initial pair distribution in the form of the Dirac delta function, designated here as Ons38-Dirac and STNH-Dirac. The well-known formula for $\Omega(F)$ based on Ons38-Dirac model [5,25] is given by

$$\Omega_{\text{Ons}}(F) = 1 - \frac{r_c}{2r_0 F} \sum_{m=1}^{\infty} P\left(m, \frac{r_c}{r_0}\right) P\left(m, \frac{2r_0 F}{r_c}\right) \quad (20)$$

where $P(m, x)$ is the incomplete gamma function of integral order m .

The analytical expression for averaged escape probability $\Omega(F)$ in the framework of STNH-Dirac model was derived by Wójcick and Tachiya [26]:

$$\Omega_{\text{NH}}(F) = 1 - \frac{r_c}{r_0} \frac{1}{\sqrt{2\pi}} \sum_{l=0}^{\infty} a_{l,0} \beta_l Z_l^2\left(\frac{2r_0}{r_c}\right) Z_l^2\left(\frac{r_c}{Fr_0}\right), \quad (21)$$

where $a_{l,0}$ are coefficients determined by Onsager T_l functions expanded into series of Legendre polynomials.

We have calculated the electric field characteristics of averaged escape probability $\Omega(F)$ according to formula (13) and some exemplary plots are displayed in Figs. 2–4. The upper horizontal axes in these figures are scaled in V/cm assuming dielectric constant $\epsilon_r = 3$ and $T = 298$ K.

Fig. 2 concerns conventional Onsager theory which assumes that geminate pairs recombine on a sphere of vanishing radius ($a = 0$). In the upper part of this figure electric field dependence of Ω is displayed: in Fig. 2a – for a Dirac delta initial pair distribution centered at various r_0 (Ons38-Dirac), and, in Fig. 2c – for a Gaussian pair distribution centered at $r_0 = 0$ with various b widths (Ons38-Gauss0). At the bottom (Fig. 2b and d) the field dependence of the ratio of escape probabilities with and without electric field, $\Omega(F)/\Omega(0)$, is plotted for the same model parameters as in the upper part of the figure. The main message from this figure is as follows. If distribution function of initial e–h pairs approaches the Dirac delta function, $\delta(r - r_0)$, and the mean intrapair distance goes to zero, $r_0 \rightarrow 0$, then, the ratio, $\Omega(F)/\Omega(0)$, approaches to the value calculated according to Eq. (22),

$$\lim_{r_0 \rightarrow 0} \frac{\Omega_{\text{Ons}}(F)}{\Omega_{\text{Ons}}(0)} = \frac{2I_1(u)}{u}, \quad (22)$$

where $u = 2\sqrt{2F}$ and $I_1(u)$ is a modified Bessel function of the first kind of the first order. In particular, we can see in Fig. 2d that the relevant curves calculated according to Ons38-Gauss0 model approach those predicted by Eq. (22) when the Gaussian distribution width goes to zero, $b \rightarrow 0$, which implies that the Gaussian function reduces to the Dirac delta function. The Eq. (22) can be derived from the expansions of $\Omega_{\text{Ons}}(F)$ for small r_0 given by Onsager (see Eq. (12) in Onsager paper [5]), Pai and Enck (see Eq. (19) in Ref. [27]), or more explicitly by Que [28] who expanded $\Omega_{\text{Ons}}(F)$ in terms of modified Bessel functions (see Eq. (7) in Ref. [28]). Interestingly, the value predicted by Eq. (22) coincides with that derived by Onsager in his earlier paper [3] from 1934 year (Onsager model designated here as Ons34) for relative increase of the dissociation constant in weak electrolytes,

$$\frac{K(F)}{K(0)} = \frac{2J_1(iu)}{iu} = \frac{2I_1(u)}{u}, \quad (23)$$

where J_1 is a Bessel function of the first order. It is worth to note here that Ons34 formula (23) concerns with bulk process in which there is a large number of ions and molecules in contrast to geminate process in which there is a single Brownian ion pair. In the Ons34 model the bulk separation of bound ion pairs (molecules) into free ions of opposite sign is assumed to be in equilibrium with the bulk recombination (assumed to be Langevin type and independent of electric field) of ions into molecules. The agreement of Ons38 formula (22) for geminate pair separation process (with $r_0 \rightarrow 0$) with the Ons34 formula (23) for bulk separation process was recognized years ago by Geacintov and Pope [29] (see also Ref. [1] page 488 and Refs. [30,31]). However, this coincidence seems to be not fully understood yet (see also [32]) because Onsager missed mathematical details in his derivation of the formula (23).

Table 1

Theoretical models of geminate recombination and their symbols used in the present paper.

Model	Final recombination sphere radius	Initial pair distribution function	Symbol
Onsager model 1938 [5]	$a = 0$	$g(r, \theta) = \frac{1}{4\pi r^2} \delta(r - r_0)$	Ons38-Dirac
		$g(r, \theta) = g_0 \exp\left(-\frac{r^2}{b^2}\right)$	Ons38-Gauss0
Sano-Tachiya–Noolandi–Hong (STNH) model [14,15]	$a > 0$	$g(r, \theta) = \frac{1}{4\pi r^2} \delta(r - r_0)$	STNH-Dirac
		$g(r, \theta) = g_0 \exp\left(-\frac{(r - r_0)^2}{b^2}\right)$	STNH-Gauss
		$g(r, \theta) = g_0 \exp\left(-\frac{ r - r_0 }{b}\right)$	STNH-Exp

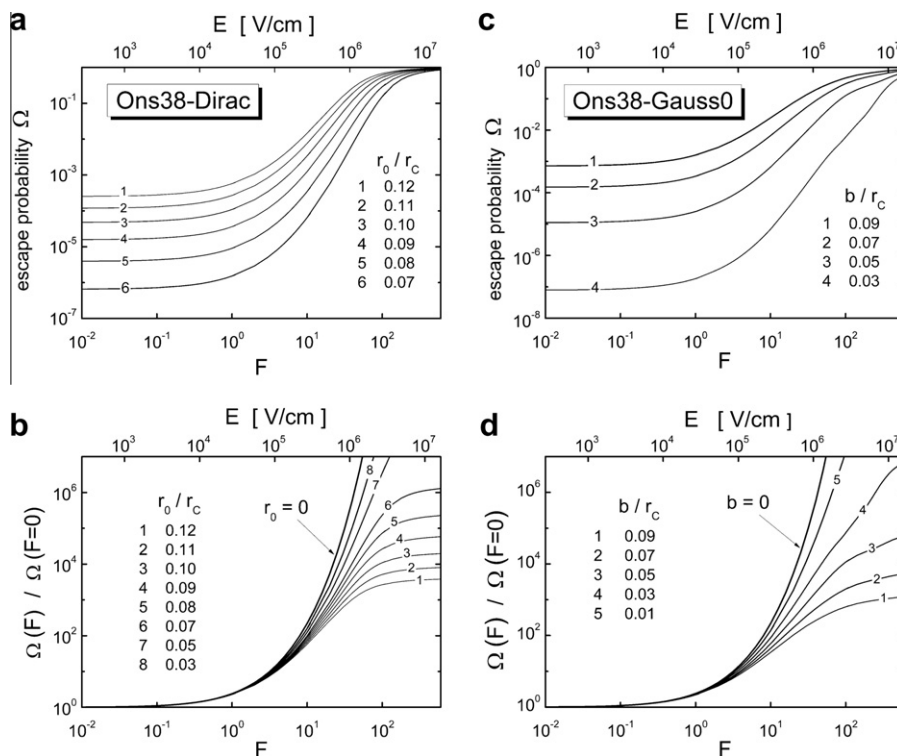


Fig. 2. Top: the dependence of averaged escape probability Ω on electric field calculated according to the Ons38-Dirac (a) and the Ons38-Gauss0 models (c) with various values of model parameters as indicated in the figure. Bottom: the dependence of the ratio, $\Omega(F)/\Omega(0)$, on electric field (b, d) obtained for the same models as displayed in the upper parts of the figure. For comparison the plots based on the Eq. (22) in Fig. 2b ($r_0 = 0$) and Fig. 2d ($b = 0$) are also displayed.

As Pope and Swenberg stated in their monumental monograph on electronic processes in organic solids [1], “this behaviour (i.e. coincidence of the formulas (22) and (23)) is to be expected since the diminishing thermalization distance (i.e. r_0) brings the ejection pattern into coincidence with the ejection pattern produced by thermal (here bulk) dissociation”.

Following Braun [33], the formula (22), due to its simplicity, is frequently used (sometimes called Braun model formula) to calculate the electric field-induced increase in dissociation probability of charge pairs in organic systems [34–40], in particular in OLEDs [35] and organic solar cells [36–40]. Braun’s approach to geminate dissociation/recombination of e–h pairs is critically analyzed in Ref. [26] where the wrong assumptions of the Braun model are recognized. The main conclusion of this reasoning is that the proper and consistent description of geminate dissociation/recombination of e–h pairs can be accomplished only on the grounds of the STNH model.

In Fig. 3 the effect of the width b of a Gaussian distribution (Fig. 3a) and exponential distribution (Fig. 3b) on escape probability in the framework of STNH theory is investigated. Calculations were performed assuming initial pair distributions centred at $r_0 = 0.1r_c$ and the following values of the final recombination parameters: $a = 0.04r_c$ and $\kappa r_c/D = 0.001$ (for typical values of r_0 and r_c in organic solids see Section 4). For either types of distribution, the wider the initial pair distribution, the larger escape probability; the effect is more remarkably seen in a low-field range. From another point of view as the width of distribution decreases to zero, the escape probability approaches the STNH-Dirac limit obtained with a distribution function in the form of the Dirac delta function. Recalling that the distribution width is a measure of the disorder of the system, we therefore state, that the disorder favours charge pair dissociation which was previously concluded by Pan and Haarer [16] on the ground of the Onsager theory.

The evident difference between STNH and Onsager theory based results can be recognized in Fig. 4 where the influence of final

recombination parameters, a and κ , on charge pair dissociation is presented. All calculations were performed assuming a Dirac delta distribution of initial e–h pairs with $r_0 = 0.1r_c$ (STNH-Dirac model). The smaller values of quenching (capture) velocity κ , the larger escape probability, the effect is more remarkably seen in a low-field range and for larger radii a of final recombination sphere which is in full agreement with recently obtained results in Ref. [26]. Comparing Figs. 3 and 4 we therefore conclude that not only disorder but also a slow rate of final recombination step can be in favour of charge pair separation. This conclusion is not trivial since electric field characteristics of escape probability are modified in a very similar way in either case. The quantitative analysis of the effect should take into account this ambiguity. Obviously, for faster final recombination proceeding on a sphere of small radius, the escape probability calculated according to the STNH-Dirac model approaches the Ons38-Dirac limit (solid lines in Fig. 4). However, we should indicate here that Noolandi–Hong statement [15] that Onsager model with $a = 0$ requires also $\kappa = \infty$ is incorrect. Onsager assumed only that the electron and hole do recombine when they approach zero distance ($a = 0$). For a zero distance, electron–hole Coulomb potential energy barrier is infinitely high and the electron cannot escape from the hole and is bound to recombine with the hole, irrespective of the value of the final recombination velocity κ . Therefore, the Onsager model corresponds to just $a = 0$ limit of the STNH model. For a non-zero but small value of recombination sphere radius, as we can see in Fig. 4c for $a = 0.03r_c$, the electric field characteristics of escape probability are rather weakly sensitive to changes in κ by orders of magnitude.

4. Comparison with experimental data

The Onsager model provides a good starting point for a quantitative description of charge photogeneration in organic solids. Here we recall results for η_0 and r_0 extracted from our previously re-

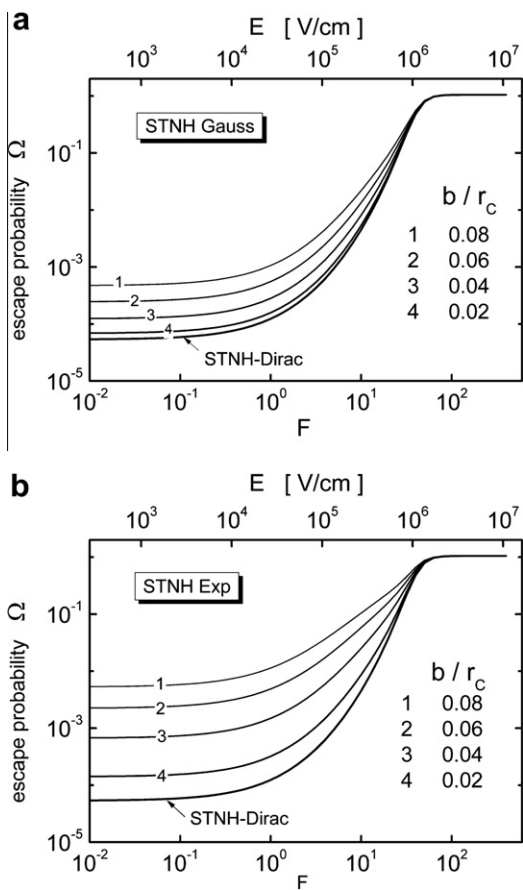


Fig. 3. Electric field characteristics of averaged escape probability obtained in the framework of the STNH-Gauss (a) and the STNH-Exp (b) models for various distribution width b . For comparison the curves based on the STNH-Dirac model are also shown. Calculations were performed assuming the following values of the model parameters: $r_0 = 0.1 r_c$, $a = 0.04 r_c$ and $\kappa r_c/D = 0.001$. For a brief description of the models see Table 1.

ported EML data for vacuum evaporated films of some organic materials. All data were analyzed consistently assuming a single value of r_0 of initial e–h pairs (Ons38-Dirac model).

For excitation in the spectral range of first low energy absorption band the r_0 radii are approximately equal to one or two specific, or two average distances in crystal lattice of investigated materials (Table 2). As concomitant polymorphism frequently occurs in organic films, in Table 2 the crystal data for the most common phases (designated by lower case Greek letters) of materials are displayed. We can notice here two types of molecular packing in crystal structures which are favourable for exciton dissociation. In the first case, crystal structures of sexithiophene (6T) [43], quinacridone (QAC) [44] and diamine derivative (TPD) [45] show layered arrangement with molecular layers (parallel to bc crystal planes) closely situated and rather separated from each other as in 6T and QAC or partly interpenetrated with phenyl rings as in TPD. The values of r_0 in this case agree well with a distance between adjacent layers (d) as in 6T and QAC or a spacing between neighbour molecules along a axis as in TPD. In the second case, the direction of “easy” dissociation in crystal lattice is established by strong coupling within a molecular stack as in solid *mer*-Alq₃ [47] or *fac*-Ir(ppy)₃ [48] where face-to-face arrangement of adjacent ligands favours the charge transfer along the c direction. In fact, the values of r_0 in either Alq₃ and Ir(ppy)₃ correspond roughly to the twice intermolecular distance along c axis indicating that the primary acts of exciton dissociation take place within the columnar stacks. A good correlation between our results for r_0 and crystallo-

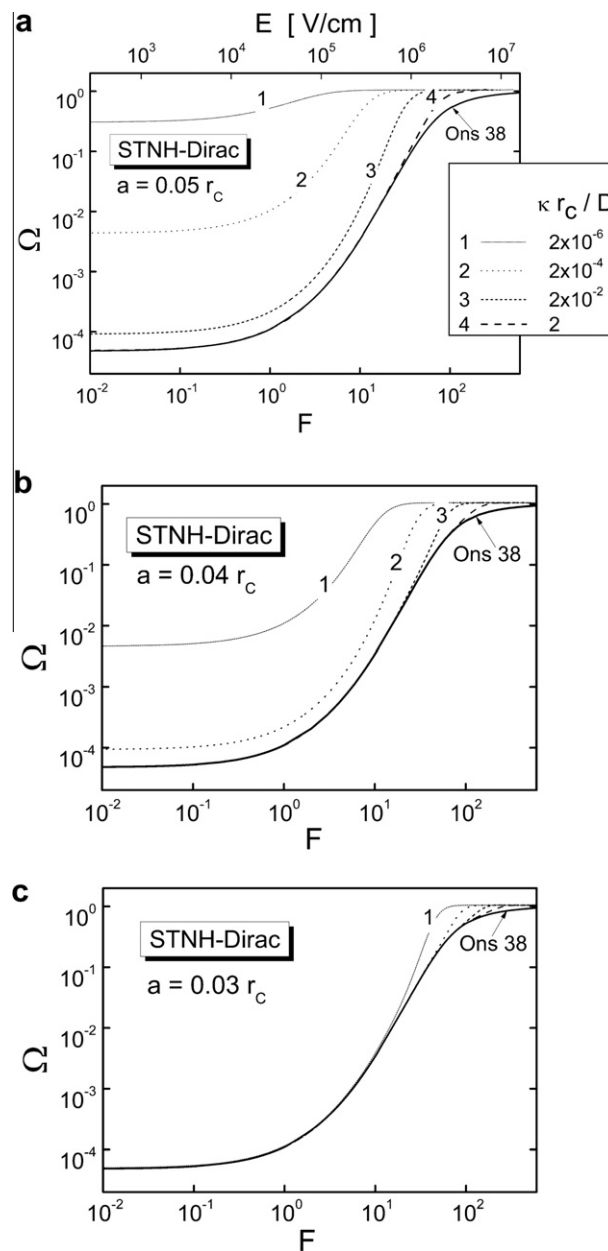
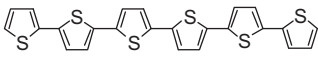
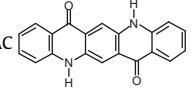
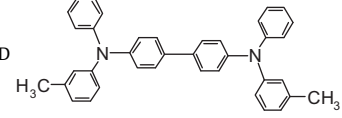
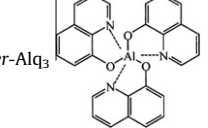
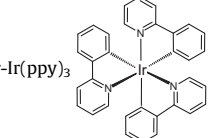


Fig. 4. Electric field characteristics of averaged escape probability obtained in the framework of the STNH-Dirac model with various values of surface recombination velocity parameter, $\kappa r_c/D$. Calculations were performed assuming $r_0 = 0.1 r_c$ and the different values of the recombination sphere radii a as indicated in the parts (a), (b) and (c) of the figure. For comparison the plots based on the Ons38-Dirac model assuming $r_0 = 0.1 r_c$ are also shown.

graphic data for materials presented in Table 2 stay in accordance with the idea that a short range order of a crystal structure is preserved in vacuum-evaporated films which is not unique but rather typical for organic films manufactured by this method (see for example [49]).

The values of primary quantum yield η_0 are ranged from 0.01 for molecules in polymer matrix [50] up to 0.8 and 0.9 for excitons in neat films Alq₃ [18] and Ir(ppy)₃ [19], respectively. Excitation of higher energy electronic states leads to both larger r_0 and η_0 [8] which agrees with thermalization mechanism of initial e–h pairs created by “hot” exciton dissociation events. The evaluated values of zero-field charge photogeneration efficiency according to the formula,

Table 2
Comparison of r_0 radii obtained according to Onsager model with available crystallographic data for selected materials.

Material	$r_0[\text{\AA}]^a$	Ref.	Sleeted crystallographic distances [\AA]	Ref.	$r_{av}[\text{\AA}]^b$
6T 	21.7–24.0	[41]	$d = 23.7$ (α phase); $d = 24.4$ (β); $d = 22.4$ (γ) along a direction	[43]	8.1
QAC 	15.7	[42]	$d = 14.2$ (α phase); $d = 15.2$ (β); $d = 13.6$ (γ) along a direction	[44]	7.0
TPD 	18.6–20.8	[8]	$a = 17.8$ (TPD); $a = 21.0$ (TPD-4)	[45] [45]	8.9 9.0
mer-Alq ₃ 	15.9	[17,18]	$c = 16.9$ (clathrate) 2×8.4 (β phase) along c direction	[46] [47]	8.5 8.1
fac-Ir(ppy) ₃ 	15.5 + 0.5	[19]	2×8.4 along c direction	[48]	8.6

^a Values of r_0 calculated according to Ons38-Dirac model from EML experimental data.

^b Average distance between molecules in crystal lattice.

$$\eta_{\text{Oms}}(F = 0) = \eta_0 \exp\left(-\frac{r_c}{r_0}\right), \quad (24)$$

are ranged from 10^{-6} to 10^{-3} which is typical for organic one-component photoconductors [1].

We note here that the Poole–Frenkel (PF) model [6,7] is rather inappropriate to describe the charge separation in organic films. In the PF formalism a charge carrier escapes from Coulomb attraction of its counterpart jumping over the potential barrier in a one step process. This assumption is difficult to realize in organic solids where the potential barrier is extended within many lattice distances ($r_c = 187 \text{\AA}$ for $\epsilon_r = 3$) and narrow bandwidths are induced by the electronic wavefunctions strongly localized in space. The explanation of the apparent success of the Onsager model originates just from the fact that it takes into account the multi-step character of charge separation process in terms of carrier diffusion. Two issues are important in this context: the nature of final recombination step and discrete character of diffusion process. The first issue is investigated in the present paper in the framework of the STNH theory assuming the final geminate recombination step proceeds on a sphere of finite radius (a) with a finite velocity (κ).

In Fig. 5 we have compared theoretical STNH results with the experimental data taken from electromodulation of photoluminescence for two archetypical organic photoconductors, Alq₃ [17,18] and Ir(ppy)₃ [19], commonly used as fluorescent (Alq₃) and phosphorescent (Ir(ppy)₃) emitters in organic LEDs [20]. Since the fast intersystem crossing ($S^* \rightarrow T^*$) induced by the heavy atom effect is considered to take place in Ir(ppy)₃ after photoexcitation, the vibrationally “hot” triplets (T^*) rather than singlet (S^*) states should be regarded as precursors of geminate e–h pairs in charge photogeneration process in Ir(ppy)₃ films (cf. [19] and references cited therein).

In EML experiments electric field-induced increase in charge separation efficiency translates into photoluminescence (PL) quenching measured usually by modulation technique at the second harmonic (2ω) of fundamental frequency (ω) of applied electric field, $E(t) = E_0 \sin(\omega t)$. The relevant quantity to be monitored is (2ω)EML signal defined as

$$(2\omega)\text{EML} = \frac{I_{2\omega}}{I_{0\omega}}, \quad (25)$$

where $I_{0\omega}$ stands for (0ω) – Fourier component and $I_{2\omega}$ – for the rms value of (2ω) – Fourier component of PL intensity I . According to the scheme displayed in Fig. 1, the PL intensity can be expressed as

$$I(E) = \frac{k_f}{k_f + k_n} [1 - \eta_0 \Omega(E)] I^*, \quad (26)$$

where I^* designates the production rate of “hot” excitons. The Fourier components of PL intensity, $I_{n\omega}$ ($n = 0, 2$), can be calculated numerically using a standard procedure [23]. As discussed in Section 1, except for the escape probability Ω , all parameters in formula (26) are assumed to be electric field independent.

In Fig. 5 the experimental electric field characteristics of (2ω) EML signals are compared with those calculated according to the STNH-Dirac model for various final recombination parameters $\kappa r_c/D$. The initial e–h separation distances r_0 were chosen on the basis of the Onsager theory as considered above. In addition, the final recombination sphere radius a was assumed to be equal to the average intermolecular distance in the crystal lattice of investigated materials (see Table 2). A reasonably good fit has been obtained with $\kappa r_c/D > 1$ for Alq₃ (Fig. 5a) and $\kappa r_c/D > 10$ for Ir(ppy)₃ (Fig. 5b). From values of $\kappa r_c/D$ we can infer capture velocities κ . To do this, diffusion coefficients were estimated using Einstein relation, $D = \mu k_B T/e$, and taking typical values of charge carrier mobility (μ) in solid Alq₃ [51] and Ir(ppy)₃ [52] as displayed in Table 3. The given values of μ refer to majority carriers which are electrons in Alq₃ and holes in Ir(ppy)₃. We estimated the lower limits of surface recombination velocity: $\kappa \cong 0.2 \text{ cm/s}$ in Alq₃ films, and $\kappa = 2 \text{ cm/s}$ in Ir(ppy)₃ films which compare favorably with an evaluation of this quantity in amorphous solids made in Refs. [21,22]. In particular, Scott and Malliaras obtained $\kappa \cong 0.6 \text{ cm/s}$ [21] for organic materials with charge carrier mobility of $10^{-5} \text{ cm}^2/\text{Vs}$ considering the mechanism of charge injection/recombination at the metal-organic solid interface in the framework of Langevin theory. We should stress here that the values of κ given above are subject to rather large uncertainty in mobility

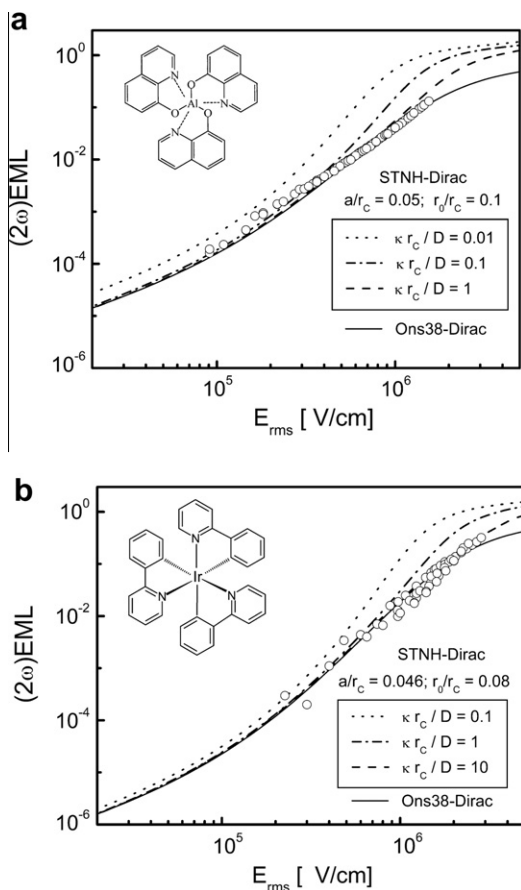


Fig. 5. A comparison of the EML experimental data (circles) with theoretical curves based on the STNH-Dirac model for three different values of capture velocity κ . The EML data for vacuum evaporated layers of Alq₃ (a) and Ir(ppy)₃ (b) are taken from Refs. [17,18] and [19], respectively. The values of the model parameters, a and r_0 , are indicated in the figure. For comparison the plots based on the Onsager-Dirac model are also shown. The abscissa of the plots stands for the rms value of the applied electric field.

Table 3
Electrical parameters for vacuum evaporated layers of Alq₃ and Ir(ppy)₃.

Material	r_c [nm]	$\frac{\kappa r_c}{D}$	μ [$\frac{\text{cm}^2}{\text{Vs}}$]	D [$\frac{\text{cm}^2}{\text{s}}$]	κ [$\frac{\text{cm}}{\text{s}}$]
Alq ₃	14.7	1	1×10^{-5a}	2.6×10^{-7}	0.2
Ir(ppy) ₃	18.7	10	1.7×10^{-5b}	4.4×10^{-7}	2

^a Reference [51].

^b Reference [52].

determination (1–2 orders of magnitude) since various methods of mobility measurements lead usually to quite different results [51]. In addition, the electric field dependence of charge carrier mobility is frequently observed in organic solids [2,53] which has not been so far implemented into diffusion equation-based formalism discussed in Section 2.

The second issue we have not here touched on is the discrete nature of the medium in which charge carrier diffusion takes place. How valid is the Onsager-based formalism of carrier continuous diffusion in organic solids was widely discussed in the context of geminate recombination on a discrete lattice using the Monte Carlo simulation method [54] and the master equation approach [55]. In particular, the dependence of the escape probability on temperature and electric field in a hopping system with a built-in Gaussian energetic disorder has been extensively studied both theoretically and experimentally by Marbourg group [56–58]. It was found that

the disorder aids dissociation and gives rise to a sub-Arrhenius-type temperature dependence [56,57]. The main reason for the effect is that at low temperatures charge carrier escape proceeds via the tail states of the DOS (density of states) which requires less thermal energy. Despite weaker temperature dependence of escape the concept of diffusion motion underlying the Onsager theory remains valid in a discrete disordered system with typical values of lattice constants. However, when modelling the field dependence of escape probability the actual r_0 distance of initial e–h pairs should be replaced by some effective distance, the effect becoming better pronounced at low temperatures [56]. In addition, the field independence of primary quantum yield (η_0) of geminate pair production might be unfulfilled as mentioned in Section 1 of this paper. A unique way to distinguish between primary exciton dissociation and subsequent dissociation of an intermediate e–h pair is the time-delayed collection field (TDCF) technique [58] which allows the simultaneous measurement of electric-field-induced fluorescence quenching and charge carrier generation efficiency. As reported for a ladder-type π -conjugated polymer [58] the EML signals induced by the field dependence of η_0 can be wrongly interpreted when applying the Onsager theory. This demonstrates that one has to be careful when performing EML data analysis.

5. Conclusions

In this paper we have studied the electric field dependence of the escape probability for various distribution functions of the initial e–h pairs in the framework of Sano–Tachiya–Noolandi–Hong model in the comparison to the conventional Onsager theory. We show that charge photogeneration is significantly enhanced, especially in a low electric field range, for larger widths of initial radii distributions of e–h pairs and smaller final recombination velocities. We compared theoretical results with the experimental data taken from electromodulation of photoluminescence (EML) for two organic photoconductors, Alq₃ and Ir(ppy)₃. From analysis of our results we infer the lower limit of final recombination velocity, $\kappa = (0.2–2)$ cm/s, in vacuum evaporated films of Alq₃ and Ir(ppy)₃ which agrees well with an evaluation of this quantity in amorphous solids.

References

- [1] M. Pope, E.C. Swenberg, *Electronic Processes in Organic Crystals and Polymers*, Oxford University Press, New York, 1999.
- [2] M. Schwoerer, H.C. Wolf, *Organic Molecular Solids*, Wiley-VCH, Weinheim, 2007.
- [3] L. Onsager, *J. Chem. Phys.* 2 (1934) 599.
- [4] L. Onsager, PhD Thesis, Yale University 1935 (also available in: *The collected works of Lars Onsager*, World Scientific, Singapore 1996).
- [5] L. Onsager, *Phys. Rev.* 54 (1938) 554.
- [6] J. Frenkel, *Phys. Rev.* 54 (1938) 647.
- [7] M.D. Tabak, P.J. Warter Jr., *Phys. Rev.* 173 (1968) 899.
- [8] W. Stampor, *Chem. Phys.* 256 (2000) 351.
- [9] W. Stampor, *Chem. Phys.* 315 (2005) 259.
- [10] V.I. Arkhipov, H. Bässler, in: W. Brütting (Ed.), *Physics of Organic Semiconductors*, Wiley-VCH, Weinheim, 2005, pp. 183–269.
- [11] J. Kalinowski, W. Stampor, P. Di Marco, *J. Chem. Phys.* 96 (1992) 4136.
- [12] S.G. Boxer, R.A. Goldstein, D.J. Lockhart, T.R. Middendorf, L. Takiff, *J. Phys. Chem.* 93 (1989) 8280.
- [13] M. Hilczler, S. Traytak, M. Tachiya, *J. Chem. Phys.* 115 (2001) 11249.
- [14] H. Sano, M. Tachiya, *J. Chem. Phys.* 71 (1979) 1276.
- [15] J. Noolandi, K.M. Hong, *J. Chem. Phys.* 70 (1979) 3230.
- [16] J. Pan, D. Haarer, *Chem. Phys. Lett.* 324 (2000) 411.
- [17] W. Stampor, J. Kalinowski, P. Di Marco, V. Fattori, *Appl. Phys. Lett.* 70 (1997) 1935.
- [18] J. Szymtowski, W. Stampor, J. Kalinowski, and Z.H. Kafafi, *Appl. Phys. Lett.* 80 (2002) 1465.
- [19] W. Stampor, J. Mężyk, *Chem. Phys.* 337 (2007) 151.
- [20] J. Kalinowski, *Organic Light-Emitting Diodes: Principles, Characteristics, and Processes*, Marcel Dekker, New York, 2005.
- [21] J.C. Scott, G. Malliaras, *Chem. Phys. Lett.* 299 (1999) 115.

- [22] L.D. Roshensteyn, A.T. Vartanyan, *Doklady Akad. Nauk. USSR* 134 (1960) 567 (in Russian).
- [23] W. Press, S.A. Teukolsky, W.T. Vetterling, B.P. Flannery, *Numerical Recipes in C: The Art of Scientific Computing*, 3rd ed., Cambridge University Press, New York, 1997.
- [24] D. Kincaid, and W. Cheney, *Numerical Analysis: Mathematics of Scientific Computing*, 3rd ed., Brooks/Cole, Pacific Grove 2002.
- [25] M. Tachiya, *J. Chem. Phys.* 89 (1988) 6929.
- [26] M. Wójcik, M. Tachiya, *J. Chem. Phys.* 130 (2009) 104107.
- [27] D.M. Pai, R.C. Enck, *Phys. Rev. B* 11 (1975) 5163.
- [28] W. Que, *Can. J. Phys.* 73 (1995) 248.
- [29] N.E. Geacintov, M. Pope, *Intrinsic Photoconductivity in Organic Crystals*, in: *Proceedings of the 3rd International Conference on Photoconductivity*, Pergamon, Oxford 1971, pp. 289–295.
- [30] K.C. Kao, W. Hwang, *Electronic Transport in Solids*, Pergamon, Oxford, 1981.
- [31] K.C. Kao, *Dielectric Phenomena in Solids*, Elsevier Academic Press, Amsterdam, 2004.
- [32] M. Hilczer, M. Tachiya, *J. Phys. Chem. C* 114 (2010) 6808.
- [33] C. Braun, *J. Chem. Phys.* 80 (1984) 4157.
- [34] J. Jung, I. Głowacki, J. Ulański, *J. Chem. Phys.* 110 (1999) 7000.
- [35] J. Kalinowski, W. Stampor, M. Cocchi, D. Virgili, V. Fattori, *Appl. Phys. Lett.* 86 (2005) 241106.
- [36] L.J.A. Koster, E.C.P. Smits, V.D. Mihailetchi, P.W.M. Blom, *Phys. Rev. B* 72 (2005) 085205.
- [37] M. Lenes, F.B. Kooistra, J.C. Hummelen, I. Van Severen, L. Lutsen, D. Vanderzande, T.J. Cleij, P.W.M. Blom, *J. Appl. Phys.* 104 (2008) 14517.
- [38] T. Offermans, S.C.J. Meskers, R.A.J. Janssen, *Chem. Phys.* 308 (2005) 125.
- [39] C. Jin, B. Pieper, B. Stiller, T. Kietzke, D. Neher, *Appl. Phys. Lett.* 90 (2007) 133502.
- [40] C. Deibel, T. Stromel, V. Dyakonov, *Phys. Rev. Lett.* 103 (2009) 036402.
- [41] J. Kalinowski, W. Stampor, P. Di Marco, F. Garnier, *Chem. Phys.* 237 (1998) 233.
- [42] J. Kalinowski, W. Stampor, P. Di Marco, *J. Electrochem. Soc.* 143 (1996) 315.
- [43] B. Servet, G. Horowitz, S. Ries, O. Lagorsse, P. Alnot, A. Yassar, F. Deloffre, P. Srivastava, R. Hajlaoui, P. Lang, F. Garnier, *Chem. Mater.* 6 (1994) 1809.
- [44] G. Lincke, H.U. Finzel, *Cryst. Res. Technol.* 31 (1996) 441.
- [45] A.R. Kennedy, W.E. Smith, D.R. Tackley, W.I.F. David, K. Shankland, B. Brown, S.J. Teat, *J. Mater. Chem.* 12 (2002) 168.
- [46] H. Schmidbaur, J. Lettenbauer, D.L. Wilkinson, G. Müller, O. Kumberger, *Z. Naturforsch. B46* (1991) 901.
- [47] M. Brinkmann, G. Gardet, M. Muccini, C. Taliani, N. Masciocchi, A. Sironi, *J. Amer. Chem. Soc.* 122 (2000) 5147.
- [48] J. Breu, P. Stossel, S. Schrader, A. Starukhin, W.J. Finkenzeller, H. Yersin, *Chem. Mater.* 17 (2005) 1745.
- [49] R. Elermann, G.M. Parkinson, H. Bässler, J.M. Thomas, *J. Phys. Chem.* 87 (1983) 544.
- [50] J. Kalinowski, W. Stampor, J. Szymkowski, D. Virgili, M. Cocchi, V. Fattori, C. Sabatini, *Phys. Rev. B* 74 (2006) 085316.
- [51] S. Barth, P. Muller, H. Riel, P.F. Seidler, W. Riess, H. Vestweber, H. Bässler, *J. Appl. Phys.* 89 (2001) 3711.
- [52] W.H. Choi, C.H. Cheung, S.K. So, *Org. Electron.* 11 (2010) 872.
- [53] P.M. Borsenberger, D.S. Weiss, *Organic Photoreceptors for Xerography*, Marcel Dekker, New York, 1998.
- [54] B. Ries, H. Schönherr, H. Bässler, M. Silver, *Phil. Mag.* 48 (1983) 87.
- [55] H. Scher, S. Rackovsky, *J. Chem. Phys.* 81 (1984) 1994.
- [56] U. Albrecht, H. Bässler, *Chem. Phys. Lett.* 235 (1995) 389.
- [57] S. Barth, D. Hertel, Y.-H. Tak, H. Bässler, H.-H. Hörhold, *Chem. Phys. Lett.* 274 (1997) 165.
- [58] D. Hertel, E.V. Soh, H. Bässler, L.J. Rothberg, *Chem. Phys. Lett.* 361 (2002) 99.